Dynamo equation solution using Finite Volume Method for midlatitude ionosphere

Feza Arikan [a], [*], Umut Sezen [a], Orhan Arikan [b]

[a] *Department of Electrical and Electronics Engineering, Hacettepe University, Ankara, Turkey*
[b] *Department of Electrical and Electronics Engineering, Bilkent University, Ankara, Turkey*

ARTICLE INFO

ABSTRACT

Ionosphere is the layer of atmosphere which plays an important role both in space based navigation, positioning and communication systems and HF signals. The structure of the electron density is a function of spatio-temporal variables. The electrodynamic medium is also influenced with earth's magnetic field, atmospheric chemistry and plasma flow and diffusion under earth's gravitation. Thus, the unified dynamo equation for the ionosphere is a second order partial differential equation for quasi-static electric potential with variable spatial coefficients. In this study, the inhomogeneous and anisotropic nature of ionosphere that can be formulated as a divergence equation is solved numerically using Finite Volume Method for the first time. The ionosphere and the operators are discretized for the midlatitude region and the solution domain is investigated for Dirichlet type boundary conditions that are built in into the diffusion equation. The analysis indicates that FVM can be a powerful tool in obtaining parametric electrostatic potential distribution in ionosphere.

1. Introduction

Ionosphere is a plasma layer that extends from 60 km to 1.000 km above earth's surface. It is anisotropic, inhomogeneous, time and space varying, and spatio-temporally dispersive in nature. Ionosphere is made up of neutral atmosphere as well as charged particles that are ionized with the solar radiation [1]. Earth's Magnetic Field (EMF) interacts with negative electrons and positive ions that are under electrical, thermodynamic and gravitational forces. The determining parameter of the ionosphere is the electron density, N_e, since electrons are significantly lighter than ions and they move with higher velocities under the EMF [2].

Ionosphere constitutes the main propagation channel for High Frequency (HF) signals that are transmitted at 3–30 MHz for communication, direction finding and Over-The-Horizon (OTH) radar systems [3]. It also plays an important role for beacon satellites operating at VHF and UHF frequency bands. At the upper end of UHF, at around 1 GHz, the impact of EMF, contributing to the anisotropicity and thus multipath phenomenon, is reduced with increasing operating frequency as compared to the highest plasma frequency of ionospheric layers. The plasma frequency is a function of electron density [4] and it is given as:

$$\omega_p = 2\pi f_p = \sqrt{\frac{e^2 N_e}{m_e \varepsilon_0}} \tag{1}$$

in rad/s, where e is the charge of an electron (1.602×10^{-19} C), m_e is the mass of an electron (9.109×10^{-31} kg) and ε_0 is the permittivity of free space ($1/36\pi \times 10^{-9}$ F/m). Because of the dependence of the refractive index to time and space derivatives, starting with L-band for operating frequencies over 1 GHz, the ionosphere still affects signals due to its dispersive nature. The higher conductivity in the ionosphere also plays a role in attenuation and absorption of uplink and downlink satellite signals especially when the ionosphere is disturbed due to geomagnetic, gravitational and seismic activities. Therefore, it is becoming an important task to understand and model the structure of ionosphere as realistically as possible.

* Corresponding author.
E-mail address: arikan@hacettepe.edu.tr (F. Arikan).

There have been various efforts in the literature to model the motion of electrons in such a complicated dynamic system as ionosphere. The magnetohydrodynamics (MHD) consists of one of the major branches of physics that is based on the induction of currents in moving conductive fluids due to magnetic fields. According to Maxwell's Equations, such currents are the vector sources of magnetic fields and due to polarization effect of the charges and moving currents, the fluid medium is polarized and thus the magnetic field is modified. Therefore, the basic set of equations that describe MHD are derived using the Navier−Stokes equations of fluid dynamics and Maxwell's equations of electromagnetism. In order to obtain the physical description of the medium, the differential equations that are stated under Navier−Stokes and Maxwell's must be solved simultaneously, either analytically or numerically [5,6]. A detailed review of possible solution methods on various geometries can be found in [7] and references therein. A typical example of convective heat transfer is given in [8], where formulated MHD equations in a controlled environment with given boundary conditions are solved using Finite Volume Method (FVM).

Although the bonds and conductivity in an ionospheric plasma are not as strong as those in a conductive fluid, the general behavior of motion of electrons and ions in a magnetoplasma such as ionosphere can still be handled using the principles of MHD [9]. Yet, the parameters that need to be determined in solution of the equation sets are very difficult to determine in the case of ionosphere due to its spatio-temporally varying nature. Thus, the researchers are forced to make approximations in order to simplify the equations, and thus reduce the unknowns and computational complexity of numerical solution methods. For example in [10], a two dimensional ionospheric potential solver is developed under the assumption of 'thin shell model'.

The constituents and concentration of the atmospheric gasses over ozone layer (after approximately 60 km in altitude) that are exposed to Extreme Ultra Violet (EUV) and X-ray radiation vary nonuniformly in height. Thus, the ion and electron densities are distributed according to the complicated thermal, electrodynamic, gravitational and magnetic forces. The electric field in the ionosphere and plasmasphere is the result of highly complicated charge movements under the influence of geomagnetic field in the magnetosphere. A detailed descriptions and initial modeling basis are provided in some early references in the literature including but not limited to [11−14]. Recently, it has been shown that the major drivers of ionospheric electric field are solar wind and its magnetic field and resulting Field Aligned Currents (FAC) [10,15−17]. The geomagnetic field and related magnetosphere plays an important role and the most commonly used International Geomagnetic Reference Field (IGRF) model is explained in detail in [18].

The general representation of continuity equation which provides the temporal rate of change of electron concentration can be summarized by the positive gain of ionization through production, negative loss due to recombination and negative change due to transport of charged particles [1]. The most common approach in modeling the behavior of charged particles is to divide the ionosphere into two basic regions. The lower layers including the D and E layers of ionosphere have higher densities of gasses and thus the generation and recombination of ions, which are mostly governed by photochemical/photoionization processes, dominate the continuity equation as discussed in detail in [1]. In the upper layers over 250 km (such as F2 layer that consists of highest plasma density), the motion of electrons and ions are mostly governed through the diffusion process and thus plasma transport component of continuity equation [1]. The region in between is known as the dynamo region [19].

Typically, the current models of terrestrial ionosphere such as Thermosphere/Ionosphere General Circulation (TIE-GCM) Model [20] and Coupled Thermosphere-Ionosphere-Plasmasphere (CTIP) Model [21] provide an incomplete representation of plasma motion especially for the dynamo region. Assimilative Mapping of Ionospheric Electrodynamics (AMIE) provides an empirical model based on multivariate regression analysis technique [17]. In [15], a global model for ionospheric potential is provided using an iterative algorithm to solve 2D continuity equations using boundary values around polar cap regions.

A more unified approach is presented in [19] where ionospheric electric field is related to the current that is generated due to both photochemical and transport processes and thus provides dynamo equation that can govern both the weak and strong magnetic field limits in the ionosphere. As opposed to other models and approaches which are mentioned above, this modeling has the potential of providing electric field behavior in vertical direction as well as horizontal.

In this study, the solution of the dynamo equation in [19] that summarizes the movement of charged particles under quasi-static and steady state ionosphere through the expression of electric potential, is formulated using Finite Volume Method [22] for probable Dirichlet and Neumann boundary values. The derivation of the differential equation for the ionospheric electrostatic potential is presented in Section 2 and the application of FVM is provided in Section 3. Section 4 consists of discussion and conclusions.

2. Derivation of differential equation for electric potential

Terrestrial ionosphere is typically modeled as a cold magnetoplasma where charged species move under gravitational as well as electric and magnetic forces [1,2,4]. Although separate equations for motion are derived for electrons and ions, the general structure for generation and recombination follows the continuity equation [1,19,23] as

$$\nabla \cdot \vec{J} + \frac{\partial \rho}{\partial t} = 0 \tag{2}$$

where $\vec{J}$ represents the volume current density and ρ is the charge density. In the quasi-static and quasi-neutral plasma, the current density can be expressed [1,19] as

$$\vec{J} = \sum_{n_s} N_{n_s} q_{n_s} \vec{v}_{n_s} \tag{3}$$

where n_s denotes the charged species ($1 \leq n_s \leq N_s$) and N_s is the total number of charged species. N_{n_s} is the number density indicating the number of charged particles of type n_s in a unit volume, q_{n_s} is the charge and $\vec{v}_{n_s}$ is the velocity of species n_s. The electric and magnetic fields can be expressed through Maxwell's Equations [19,23] as:

$$\nabla \times \vec{E} = 0 \tag{4}$$

$$\nabla \times \vec{H} = \mu_0 \vec{J} \tag{5}$$

$$\nabla \cdot \vec{B} = 0 \tag{6}$$

where $\vec{E}$ and $\vec{H}$ denote the electric and magnetic field strengths, respectively. $\vec{B}$ is the magnetic flux density, and μ_0 is the permeability of free space ($4\pi \times 10^{-7}$ H/m), where $\vec{B} = \mu_0 \vec{H}$. In the above equations, $\cdot$ and $\times$ denote the dot and cross products, respectively,

and ∇ is the gradient operator. The fourth Maxwell's Equation corresponding to the Gauss' Law for electricity is satisfied with

$$\sum_{n_s} N_{n_s} q_{n_s} = 0 \tag{7}$$

under quasi-neutrality [19].

One of the basic representations is the conservation of momentum for each species of charged particles that are in a plasma environment as given in [24] and [25]:

$$
\begin{aligned}
m_{n_s}\frac{\partial \overrightarrow{v}_{n_s}}{\partial t} + m_{n_s}(\overrightarrow{v}_{n_s}\cdot\nabla)\overrightarrow{v}_{n_s} = {} & m_{n_s}\overrightarrow{g} - \frac{1}{N_{n_s}}\nabla(N_{n_s}kT_{n_s}) + q_{n_s}\overrightarrow{E} + q_{n_s}\overrightarrow{v}_{n_s}\times\overrightarrow{B} \\
& - m_{n_s}\nu_{n_s;n}(\overrightarrow{v}_{n_s} - \overrightarrow{u}) \\
& - m_{n_s}\left(\sum_{n_s\neq n_p}\nu_{n_s;n_p}(\overrightarrow{v}_{n_s} - \overrightarrow{v}_{n_p})\right)
\end{aligned}
\tag{8}
$$

where m_{n_s} denotes the mass of charged species; $\overrightarrow{u}$ is the neutral wind velocity; $\overrightarrow{g}$ is the acceleration due to gravity; and T_{n_s} is the temperature of the charge of species n_s. k is the Boltzmann's constant (1.381×10^{-23} J K^{-1}). $\nu_{n_s;n}$ and $\nu_{n_s;n_p}$ denote the diffusion collision frequencies for collisions between the species n_s and the neutral particles and species n_p, respectively.

Under quasi-static and quasi-neutral approximations for cold magnetoplasma, the left hand side of (8) is assumed to be zero, and the effects of collisions between charged particles are neglected [19]. Under these assumptions and approximations, (8) can be rewritten as:

$$0 = m_{n_s}\overrightarrow{g} - \frac{1}{N_{n_s}}\ \nabla(N_{n_s}kT_{n_s}) + q_{n_s}\overrightarrow{E'} + q_{n_s}B\underline{\underline{\Delta}}\ \overrightarrow{w}_{n_s} - m_{n_s}\nu_{n_s;n}\overrightarrow{w}_{n_s} \tag{9}$$

where

$$\overrightarrow{w}_{n_s} = \overrightarrow{v}_{n_s} - \overrightarrow{u} \tag{10}$$

$$\overrightarrow{B} = B\widehat{b} \tag{11}$$

$$\overrightarrow{E'} = \overrightarrow{E} + \overrightarrow{u}\times\overrightarrow{B} \tag{12}$$

and

$$\underline{\underline{\Delta}} = \begin{bmatrix} 0 & +b_z & -b_y \\ -b_z & 0 & +b_x \\ +b_y & -b_x & 0 \end{bmatrix}. \tag{13}$$

Now, (3) can be modified and the current density can be given in terms of above definitions [19] as

$$\overrightarrow{J} = \sum_{n_s} N_{n_s} q_{n_s} \overrightarrow{w}_{n_s}. \tag{14}$$

When the above equation is linearized to provide a relationship between the current density and $\overrightarrow{E'}$, the following equation can be derived as detailed in [19]:

$$\overrightarrow{J} = \overrightarrow{Q} + \underline{\underline{S}}\overrightarrow{E'} \tag{15}$$

where

$$\overrightarrow{Q} = \sum_{n_s}\frac{N_{n_s}q_{n_s}}{m_{n_s}\nu_{n_s;n}}(\underline{\underline{I}} - \kappa_{n_s}\underline{\underline{\Delta}})^{-1}\left(m_{n_s}\overrightarrow{g} - \frac{1}{N_{n_s}}\nabla(N_{n_s}kT_{n_s})\right) \tag{16}$$

and

$$\underline{\underline{S}} = \sum_{n_s}\frac{N_{n_s}q_{n_s}^2}{m_{n_s}\nu_{n_s;n}}(\underline{\underline{I}} - \kappa_{n_s}\underline{\underline{\Delta}})^{-1}. \tag{17}$$

The κ_{n_s} denotes the ratio of gyrofrequency ($|q_{n_s}|B/m_{n_s}$) to the collision frequency, $\nu_{n_s;n}$. κ_{n_s} has the same sign as q_{n_s}. Although $\underline{\underline{\Delta}}$ is a non-invertible matrix, $(\underline{\underline{I}} - \kappa_{n_s}\underline{\underline{\Delta}})$ is invertible for all $\kappa_{n_s}\neq\infty$ as explained in detail in [19]. κ_{n_s} plays a crucial role in directions of components of current density both for $\overrightarrow{Q}$ and $\underline{\underline{S}}\overrightarrow{E'}$ for all charge type n_s. If $\kappa_{n_s}\ll1$, it is called the weak field condition and the gravitational and pressure gradient forces are in vertical direction. If $\kappa_{n_s}\gg1$, it is called the strong field condition and both $\overrightarrow{Q_{n_s}}$ and $\underline{\underline{S}}_{n_s}\overrightarrow{E'}$ are parallel to $\overrightarrow{B}$.

Using quasi-static and steady state approximations in (4), the electric field can be represented as the gradient of scalar potential, Φ [23], as:

$$\overrightarrow{E} = -\nabla\Phi. \tag{18}$$

Also, in (2), the derivative of charge density is assumed to be zero and the definition in (15) can be replaced for the current density as:

$$\nabla\cdot\overrightarrow{J} = 0 \tag{19}$$

$$\nabla\cdot\left(\overrightarrow{Q} + \underline{\underline{S}}\overrightarrow{E'}\right) = 0 \tag{20}$$

$$\nabla\cdot\left(\overrightarrow{Q} + \underline{\underline{S}}(\overrightarrow{E} + \overrightarrow{u}\times\overrightarrow{B})\right) = 0 \tag{21}$$

$$\nabla\cdot\left(\overrightarrow{Q} + \underline{\underline{S}}(-\nabla\Phi + \overrightarrow{u}\times\overrightarrow{B})\right) = 0 \tag{22}$$

$$\nabla\cdot\left(\overrightarrow{Q} - \underline{\underline{S}}\nabla\Phi + B\underline{\underline{S}}\ \underline{\underline{\Delta}}\ \overrightarrow{u}\right) = 0 \tag{23}$$

This final form of differential equation can be solved numerically for a defined region of ionosphere under the given boundary values as described in the next section. Once the potential is determined,

the electric field and the current density can be obtained for the same region of interest by using (15) and (18).

3. Application of Finite Volume Method to the solution of electrostatic potential

Finite Volume Method (FVM) is a numerical method for computation of partial differential equations that are converted into the form of algebraic equations that are constructed around the small volumes (voxels) that constitute the main volume of interest [22]. FVM is based on representation of volume integrals in a partial differential equation that contain a divergence term in terms of surface integral, which in term, is computed around discretized surfaces of the individual voxel that are called the faces. The conversion from the volume integral to the surface integral is achieved using the Divergence Theorem [8,22,23]. As compared to other implementations of finite element and finite difference methods, FVM inherently ensures the conservation of physical parameter of interest even for unstructured meshes [7,22].

The application of FVM to the solution of ionospheric electrostatic potential starts with (23) which is defined in a volume $V(\vec{r})$, where $\vec{r}$ is the position vector in the defined coordinate system [23]. The first step of FVM consists of the discretization of volume of interest $V(\vec{r})$ into smaller volumes called the voxels in a general coordinate system defined by unit vectors $(\hat{a}_{n1}, \hat{a}_{n2}, \hat{a}_{n3})$. The initial point of the volume is defined as $c_i(c_{in1}, c_{in2}, c_{in3})$ and the final point of the volume can be given as $c_e(c_{en1}, c_{en2}, c_{en3})$. The discretization of the volume in 3-D can be accomplished by defining the number of partitions in each direction and the distance between each partition in the given direction as:

$$\Delta(n1) = \frac{|c_{en1} - c_{in1}|}{N_{n1}} \tag{24}$$

$$\Delta(n2) = \frac{|c_{en2} - c_{in2}|}{N_{n2}} \tag{25}$$

$$\Delta(n3) = \frac{|c_{en3} - c_{in3}|}{N_{n3}} \tag{26}$$

where $\Delta(n1)$, $\Delta(n2)$ and $\Delta(n3)$ denote the distance between two neighboring voxels and N_{n1}, N_{n2} and N_{n3} represent the total number of voxels in dimensions $n1$, $n2$ and $n3$, respectively.

In the application of FVM, when the cell-centered approach is implemented [22], each voxel can be uniquely identified using a lexicographical index l as

$$l = n_1 + N_{n1}(n_2 - 1) + N_{n1}N_{n2}(n_3 - 1) \tag{27}$$

where $1 \leq l \leq N_{n1}N_{n2}N_{n3}$. The indices n_1, n_2 and n_3 indicate the voxel number in the direction of $n1$, $n2$, and $n3$, respectively. The indices are defined in the ranges as $1 \leq n_1 \leq N_{n1}$, $1 \leq n_2 \leq N_{n2}$, and $1 \leq n_3 \leq N_{n3}$. The center of voxel l is defined as $c_l(c_{ln1}, c_{ln2}, c_{ln3})$.

The volume of interest $V(\vec{r})$ is approximated as the collection of $N_{n1}N_{n2}N_{n3}$ voxels as

$$V(\vec{r}) \simeq \sum_{l=1}^{N_{n1}N_{n2}N_{n3}} V_l(\vec{r}) \tag{28}$$

where $V_l(\vec{r})$ denotes the volume of voxel l. The surface of the volume defined by $V_l(\vec{r})$ can be expressed as a collection of two dimensional smaller surfaces called as faces as:

$$S_l(\vec{r}) \simeq \sum_{n_f=1}^{N_f} S_{l;n_f}(\vec{r}) \tag{29}$$

where $S_l(\vec{r})$ denotes the surface function of voxel l surrounding the volume $V_l(\vec{r})$ and $S_{l;n_f}(\vec{r})$ indicate the 2-D surfaces that approximate surface $S_l(\vec{r})$ for N_f number of faces, where $1 \leq n_f \leq N_f$. In the case of ionosphere, where the volume is a plasma environment bounded by mathematical user-defined surfaces, (29) can be considered as exact.

The second step of FVM constitutes the transformation of the differential equation given in (23) into an algebraic set of equation defined in partitioned volume of interest. Therefore, the volume integral of the divergence equation in (23) is taken as

$$\int_{V(\vec{r})} \nabla \cdot \left(\vec{Q} - \underline{\underline{S}} \nabla \Phi + B\underline{\underline{S}} \underline{\underline{\Delta}} \vec{u} \right) dv = 0. \tag{30}$$

The divergence operator and its volume integral given in (30) is valid for all individual voxel volumes $V_l(\vec{r})$ that make up total volume $V(\vec{r})$. Then, the volume integral of divergence in each individual voxel can be expressed as, $\forall l$:

$$\int_{V_l(\vec{r})} \nabla \cdot \left(\vec{Q} - \underline{\underline{S}} \nabla \Phi + B\underline{\underline{S}} \underline{\underline{\Delta}} \vec{u} \right) dv = 0 \tag{31}$$

that can be converted to a surface integral using the Divergence Theorem as:

$$\oint_{S_l(\vec{r})} \left(\vec{Q} - \underline{\underline{S}} \nabla \Phi + B\underline{\underline{S}} \underline{\underline{\Delta}} \vec{u} \right) \cdot d\vec{A} = 0 \tag{32}$$

where $d\vec{A}$ denotes the differential surface element. The above surface integral can now be discretized over the faces of voxel l, $\forall l$ as:

$$\sum_{n_f=1}^{N_f} \left(\vec{Q} - \underline{\underline{S}} \nabla \Phi + B\underline{\underline{S}} \underline{\underline{\Delta}} \vec{u} \right) \cdot \hat{a}_{l;n_f} \Delta A_{l;n_f} = 0 \tag{33}$$

where $\hat{a}_{l;n_f}$ and $\Delta A_{l;n_f}$ define the surface unit normal and surface area for voxel l and face n_f, respectively.

Once the volume of interest $V(\vec{r})$ and the surface of voxel l, $S_l(\vec{r})$, are discretized as described in the above equations, (33) can be rewritten as

$$\sum_{n_f=1}^{N_f} \left((\nabla \Phi)^T \underline{\underline{S}}^T \right) \hat{a}_{l;n_f} = \sum_{n_f=1}^{N_f} \underbrace{\left(\vec{Q} + B\underline{\underline{S}} \underline{\underline{\Delta}} \vec{u} \right)^T \hat{a}_{l;n_f}}_{p_{l;n_f}} \tag{34}$$

where T denotes the transpose operator. The second step of application of FVM consists of the discretization of $(\nabla \Phi)^T \underline{\underline{S}}^T \hat{a}_{l;n_f}$ for each voxel l. The basic assumption in the discretization process as given in [22] is the computation to be done over the centroid line that connects voxel l to its neighbor in the direction of $\hat{a}_{l;n_f}$ over the face n_f in the cell-centered approach using the finite difference techniques.

Starting with

$$\underline{\underline{S}}^T \hat{a}_{l;n_f} = \vec{k}_{l;n_f} \tag{35}$$

$$= k_{l;n_f} \hat{a}_{l;n_f} \tag{36}$$

$$= \sum_{n_d=1}^{3} k_{l;n_f}(n_d) \widehat{a}_{n_d} \qquad (37)$$

where $n_d = n_1$, n_2, n_3. Then, the inner computations of (34) for each face can be approximated as

$$(\nabla\Phi)^T \underline{\underline{S}}^T \widehat{a}_{l;n_f} \simeq \sum_{n_d=1}^{3} k_{l;n_f}(n_d) \frac{\Phi(c_{l;n_d}) - \Phi(c_l)}{|\overrightarrow{r}_{l;n_d} - \overrightarrow{r}_l|} \qquad (38)$$

where $\Phi(c_l)$ denotes the value of potential at the center point of voxel l, and $\Phi(c_{l;n_d})$ is the value of potential at the center point of

$$\underline{\Phi} = [\Phi(1)\ldots\Phi(l)\ldots\Phi(N_{n1}N_{n2}N_{n3})]^T, \qquad (44)$$

and $\Phi(l)$ denotes $\Phi(c_l)$. Also,

$$\underline{P} = \left[p_1\ldots p_l\ldots p_{N_{n1}N_{n2}N_{n3}}\right]^T, \qquad (45)$$

and

$$\underline{\underline{D}} = \left[\underline{d}_1\ldots\underline{d}_l\ldots\underline{d}_{N_{n1}N_{n2}N_{n3}}\right]. \qquad (46)$$

The vectors $\underline{d}_l$ contain the coefficients that are given (39), (40) and (42). The matrix $\underline{\underline{D}}$ is a square sparse matrix of size $N_{n1}N_{n2}N_{n3} \times N_{n1}N_{n2}N_{n3}$.

The boundary voxels are defined as those for $n_3 = 1,\ldots,N_{n3}$

Back $\rightarrow$ $l = N_{n1}N_{n2}(n_3 - 1) + N_{n1} : N_{n1} : N_{n1}N_{n2}n_3$
Front $\rightarrow$ $l = N_{n1}N_{n2}(n_3 - 1) + 1 : N_{n1} : N_{n1}N_{n2}(n_3 - 1) + N_{n1}(N_{n2} - 1) + 1$
Left $\rightarrow$ $l = N_{n1}N_{n2}(n_3 - 1) + 1 : 1 : N_{n1}N_{n2}(n_3 - 1) + N_{n1}$
Right $\rightarrow$ $l = N_{n1}N_{n2}(n_3 - 1) + N_{n1}(N_{n2} - 1) + 1 : 1 : N_{n1}N_{n2}n_3$
Bottom $\rightarrow$ $l = 1 : 1 : N_{n1}N_{n2}$
Top $\rightarrow$ $l = N_{n1}N_{n2}(N_{n3} - 1) + 1 : 1 : N_{n1}N_{n2}N_{n3}$

$$(47)$$

neighbor voxel in the direction of n_d. $\overrightarrow{r}_l$ and $\overrightarrow{r}_{l;n_d}$ are the position vectors to the center point of voxel l and its neighbor voxel in the direction of n_d. Thus, $|\overrightarrow{r}_{l;n_d} - \overrightarrow{r}_l|$ is the distance between the center point of voxel l and the center point of its neighbor voxel in the direction of n_d.

Equation (34) can be rewritten by changing the order of summations after the application of approximation on the gradient of the potential as:

$$\sum_{n_d=1}^{3} \frac{\Phi(c_{l;n_d}) - \Phi(c_l)}{|\overrightarrow{r}_{l;n_d} - \overrightarrow{r}_l|} \underbrace{\sum_{n_f=1}^{N_f} k_{l;n_f}(n_d)}_{\alpha_{l;n_d}} = \sum_{n_f=1}^{N_f} p_{l;n_f} \qquad (39)$$

Let us define

$$\beta_{l;n_d} = \alpha_{l;n_d} \frac{1}{|\overrightarrow{r}_{l;n_d} - \overrightarrow{r}_l|} \qquad (40)$$

and (39) can be expressed as

$$-\Phi(c_l)\gamma_l + \sum_{n_d=1}^{3} \beta_{l;n_d}\Phi(c_{l;n_d}) = \underbrace{\sum_{n_f=1}^{N_f} p_{l;n_f}}_{p_l} \qquad (41)$$

where

$$\gamma_l = \sum_{n_d=1}^{3} \beta_{l;n_d}. \qquad (42)$$

The third step of FVM requires the algebraic expression of the approximated differential equation. (39) can be represented in a set of linear equations as:

$$\underline{\underline{D}}^T \underline{\Phi} = \underline{P} \qquad (43)$$

where

Thus, in this case, the value of the electrostatic potential on the boundaries can be estimated using the entries of $\underline{P}$, p_l, for those voxels l on the boundaries given in (47). This kind of boundary condition can be classified as Dirichlet type. The solution can be considered to be accurate to the second order as given in detail in [22]. On the boundaries, the gradient in (38) is approximated towards the inner volume in the directions of $-\widehat{a}_{n_d}$. The solution for the ionospheric electrostatic potential can be obtained in the least square sense as:

$$\underline{\widetilde{\Phi}} = \left(\underline{\underline{D}}\,\underline{\underline{D}}^T\right)^{-1} \underline{\underline{D}}\,\underline{P} \qquad (48)$$

The solution given in (48) can be obtained for any volume of interest in the ionosphere either midlatitude, equatorial or high latitude as long as the model parameters sufficiently represent the underlying structure of ionosphere.

3.1. Application to ionospheric volume of interest

The volume of interest in the ionosphere is defined using Earth Centered Earth Fixed (ECEF) coordinate system, using the spherical voxels. The volume of interest is partitioned in spherical unit vectors ($\widehat{a}_r$, $\widehat{a}_\theta$, $\widehat{a}_\phi$). The voxel centers and the position vectors to the voxel centers are expressed in Cartesian coordinate system as $\overrightarrow{r} = x\widehat{a}_x + y\widehat{a}_y + z\widehat{a}_z$ and $c_l(c_{lx}, c_{ly}, c_{lz})$.

The physical parameters that are necessary to compute the values of $\overline{\overline{Q}}$, $\underline{S}$, $B\underline{\lambda}$ and $\overrightarrow{u}$ can obtained from empirical ionospheric models such as International Reference Ionosphere (IRI) as given in www.irimodel.org [26], Horizontal Wind Model (HWM07) [27], MSIS-e−90 atmosphere model given in https://cohoweb.gsfc.nasa.gov/vitmo/msis_vitmo.html [28] and International Geomagnetic Reference Field (IGRF) (http://www.geomag.bgs.ac.uk/data_service/models_compass/igrf.html).

For a given coordinate, date and time, the above mentioned models provide the parameters of neutral and ionized particles, ion and electron temperatures and number densities, and EMF direction and magnitude. An example of model derived parameter set that will be used in dynamo equation solution is provided in Fig. 1. For Ankara, Turkey (39.89° N, 32.76° E), on 21 March, 2011 (equinox
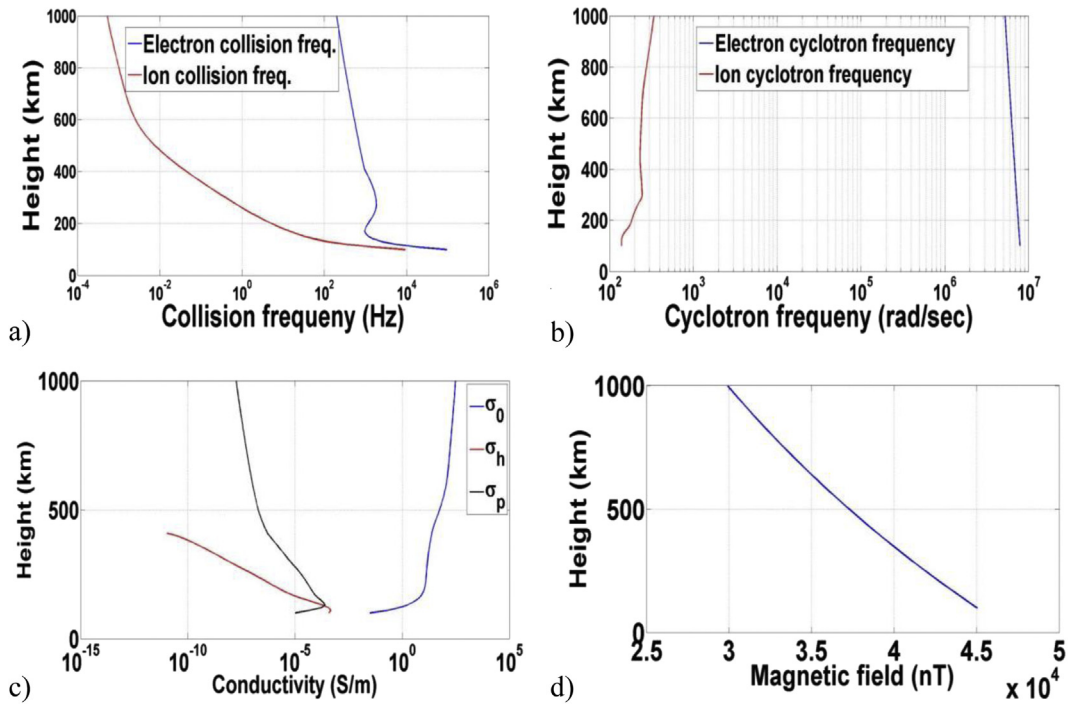
Fig. 1. a) Electron (blue) and ion (red) collision frequencies, b) Electron (blue) and ion (red) cyclotron frequencies, c) Direct (or longitudinal) (blue), Hall (red) and Pedersen (or transversal) (black) conductivities and magnetic field magnitude for Ankara, Turkey (39.89° N, 32.76° E) on 21 March, 2011 at 12:00 LT.

day) at 12:00 LT, the electron (blue line) and ion (red line) collision frequencies are provided in Fig. 1a. The corresponding cyclotron frequencies are given in Fig. 1b for electron (blue line) and ion (red line). The conductivities that are necessary to understand the complex dielectric permittivities are provided in Fig. 1c, where direct (or longitudinal) Hall and Pedersen (or transversal)

conductivities are indicated with blue, red and black lines, respectively. The geomagnetic field magnitude (or intensity) over Ankara is drawn in Fig. 1d using the IGRF model.

The main component of all equations rely on electron and ion number densities and contour plots N_e are provided in Fig. 2 for (39° N, 35° E) on a quiet day of September 1, 2011 (Fig. 2a,b,c) and also
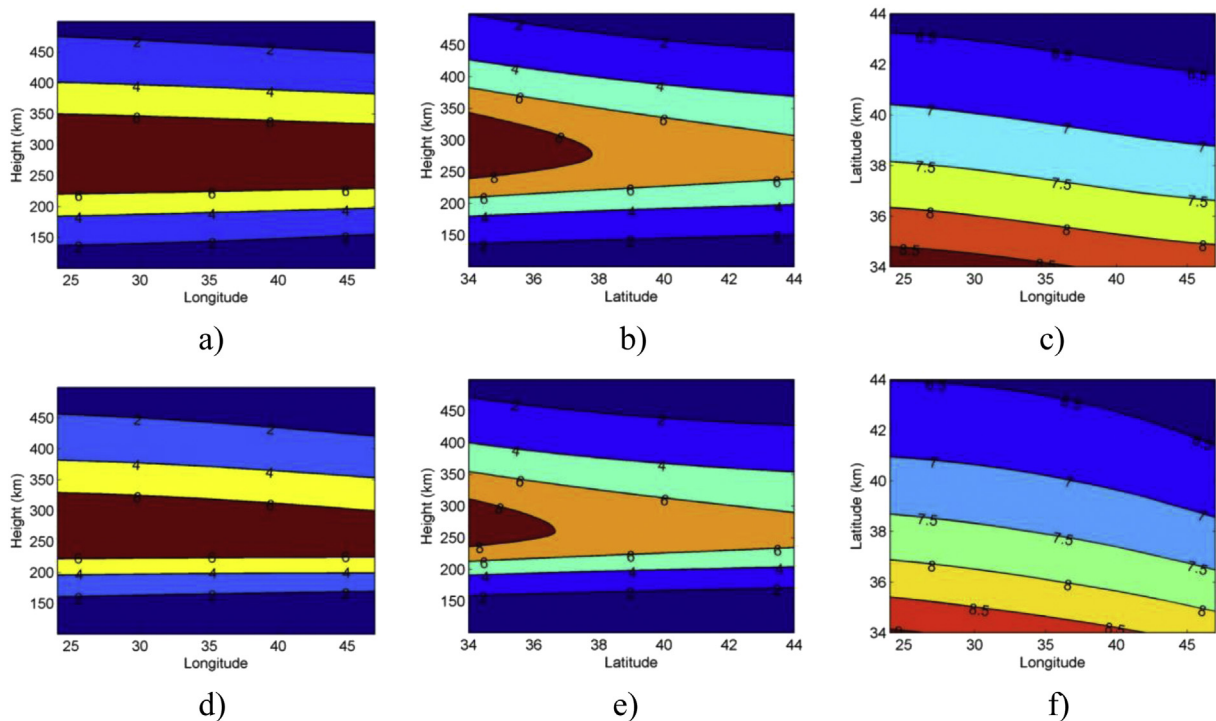

Fig. 2. Electron density contours obtained from IRI-Plas; on September 1, 2011 (geomagnetically quiet day) at 14:00 LT a) fixed latitude of 39° N, b) fixed longitude of 35° E, c) fixed height of 250 km; on March 10, 2011 (positively disturbed storm day) at 14:00 LT d) fixed latitude of 39° N, e) fixed longitude of 35° E, f) fixed height of 250 km.

on a geomagnetically (positively) disturbed day of 10 March 2011 (Fig. 2d,e,f) at 14:00 LT. Fig. 2a,d are drawn on a fixed latitude of 39° N, longitude and height are variables; Fig. 2b,e are drawn on a fixed longitude of 35° E, latitude and height are variables; and Fig. 2c,f are drawn on at a fixed height of 250 km, latitude and longitude are variables. The model values are obtained from International Reference Ionosphere extended to Plasmasphere (IRI-Plas) model as given in [29] using the online computational form at www.ionolab.org. In the application of the IRI-Plas model, no external inputs are given. Thus, as it can be observed from Fig. 2 that the model does not differentiate between a calm day and a geomagnetically disturbed day without any additional information. The electron density contours are very similar to each other for any projection.

Using the inputs from the models similar to those given above, the estimates for the approximate potential distribution in the voxel centers can be computed using (48). After the estimation of potential distribution, the electric field can be obtained using (18). After the computation of $\vec{E}$ in (12), the current density $\vec{J}$ in (15) can be obtained. Since the realistic values or the measurement values are very difficult to obtain (as discussed in [11,14,30]), such a simulation environment constitutes a major contribution in understanding the structural ionospheric physics. Detailed simulations and analysis will be posed as a future work.

4. Discussion and conclusion

The conservation of momentum is a defining relationship for generation and recombination of ions in cold plasma. Solar radiation and wind from above, and Earth's magnetic and gravitational fields from below force the charged particles in continuous motion. With the derivation of dynamo equation for a steady state ionosphere under quasi neutrality in [19], the representation of charged particle behavior from bottom side to top side of ionosphere is made possible for the first time. In this study, the electrostatic potential formulated using the dynamo equation is solved using Finite Volume Method for terrestrial ionosphere. The problem formulation of dynamo equation inherently satisfies the built-in Dirichlet type boundary values. The solution can be considered to be valid as long as the model parameter values provide a fair representation for the state of ionosphere. In future studies, the solution for electrostatic potential will be compared with limited experimental measurement campaign results that are obtained by Low Earth Orbit (LEO) satellites.

References

[1] H. Rishbeth, O.K. Garriott, Introduction to Ionospheric Physics, International Geophysics Series, vol. 14, Academic Press, New York, NY, 1969.
[2] K. Davies, Ionospheric Radio, Peter Peregrinus Ltd., IET, London, 1990.
[3] J.M. Goodman, HF Communication: Science & Technology, Van Nostrand Reinhold Company, 1992.
[4] J.K. Hargreaves, The Solar-terrestrial Environment, Cambridge Atmospheric and Space Science Series, Cambridge University Press, 1992.
[5] T.G. Cowling, Magnetohydrodynamics, Interscience, New York, NY, 1957.
[6] R.J. Moreau, Magnetohydrodynamics, vol. 3, Springer Science & Business Media, e-book, 2013.
[7] M. Sheikholeslami, D.D. Ganji, Nanofluid convective heat transfer using semi analytical and numerical approaches: a review, J. Taiwan Inst. Chem. Eng. 65 (2016) 43–77.
[8] F. Garoosi, L. Jahanshaloo, M.M. Rashidi, A. Badakhsh, M.E. Ali, Numerical simulation of natural convection of the nanofluid in heat exchangers using a Buongiorno model, Appl. Math. Comput. 254 (2015) 183–203.
[9] B.N. Gershman, Dynamics of the Ionospheric Plasma, Izdatel'stvo Nauka, Moscow, 1974.
[10] A. Nakamizo, Y. Hiraki, Y. Ebihara, T. Kikuchi, K. Seki, T. Hori, A. Ieda, Y. Miyoshi, Y. Tsuji, Y. Nishimura, A. Shinbori, Effect of R2-FAC development on the ionospheric electric field pattern deduced by a global ionospheric potential solver, J. Geophys. Res. Space Phys. 117 (A9) (2012).
[11] R.L.F. Boyd, Measurement of electric fields in the ionosphere and magneto-sphere, Space Sci. Rev. 7 (2–3) (1967) 230–237.
[12] Y. Kamide, A.D. Richmond, S. Matsushita, Estimation of ionospheric electric fields, ionospheric currents, and field-aligned currents from ground magnetic records, J. Geophys. Res. Space Phys. 86 (A2) (1981) 801–813.
[13] M.I. Pudovkin, Electric fields and currents in the ionosphere, Space Sci. Rev. 16 (5–6) (1974) 727–770.
[14] R. Lukianova, F. Christiansen, Modeling of the global distribution of ionospheric electric fields based on realistic maps of field-aligned currents, J. Geophys. Res. Space Phys. 111 (A3) (2006).
[15] R.Y. Lukianova, Electric potential in the earth's ionosphere: a numerical model, Math. Models Comput. Simul. 9 (6) (2017) 708–715.
[16] A.A. Namgaladze, M. Förster, B.E. Prokhorov, O.V. Zolotov, Electromagnetic drivers in the upper atmosphere: observations and modeling, in: The Atmosphere and Ionosphere (pp. 165–219), Springer, Dordrecht, 2013.
[17] A.J. Ridley, G. Crowley, C. Freitas, An empirical model of the ionospheric electric potential, Geophys. Res. Lett. 27 (22) (2000) 3675–3678.
[18] A. Chambodut, Geomagnetic field, IGRF, in: Encyclopedia of Solid Earth Geophysics (pp. 379–380), Springer Netherlands, 2011.
[19] P. Withers, Theoretical models of ionospheric electrodynamics and plasma transport, J. Geophys. Res. Space Phys. 113 (A7) (July 2008) 1–12.
[20] A.D. Richmond, E.C. Ridley, R.G. Roble, A thermosphere/ionosphere general circulation model with coupled electrodynamics, Geophys. Res. Lett. 9 (6) (March 1992) 601–604.
[21] G.H. Millward, R.J. Moffett, S. Quegan, T.J. Fuller-Rowell, A coupled thermosphere-ionosphere-plasmasphere model (CTIP), in: STEP Handbook on Ionospheric Models, 1996, pp. 239–279.
[22] F. Moukalled, L. Mangani, M. Darwish, The Finite Volume Method in Computational Fluid Dynamics, Springer, e-book, 2016.
[23] J.A. Kong, Electromagnetic Wave Theory, John Wiley & Sons, New York, NY, 1986.
[24] S. Chandra, Plasma diffusion in the ionosphere, J. Atmos. Sol. Terr. Phys. 26 (1964) 113–122.
[25] P.M. Banks, G. Kockarts, Aeronomy, Elsevier, New York, NY, 1973.
[26] D. Bilitza, D. Altadill, Y. Zhang, C. Mertens, V. Truhlik, P. Richards, L.-A. McKinnell, B. Reinisch, The International Reference Ionosphere 2012 -– a model of international collaboration, J. Space Weather Space Clim. 4 (A07) (2014) 1–12.
[27] D.P. Drob, J.T. Emmert, G. Crowley, J.M. Picone, G.G. Shepherd, W. Skinner, P. Hays, R.J. Niciejewski, M. Larsen, C.Y. She, J.W. Meriwether, G. Hernandez, M.J. Jarvis, D.P. Sipler, C.A. Tepley, M.S. O'Brien, J.R. Bowman, Q. Wu, Y. Murayama, S. Kawamura, I.M. Reid, R.A. Vincent, An empirical model of the Earth's horizontal wind fields: HWM07, J. Geophys. Res. Space Phys. 113 (A12304) (2008) 1–18.
[28] A. E. Hedin, Extension of the MSIS thermospheric model into the Middle and lower atmosphere, J. Geophys. Res. 96(1159), 1991.
[29] U. Sezen, T.L. Gulyaeva, F. Arikan, Performance of solar proxy options of IRI-Plas model for equinox seasons, J. Geophys. Res. Space Phys. (123) (2018) 1441–1456, https://doi.org/10.1002/2017JA024994.
[30] C. Yang, B. Zhao, J. Zhu, X. Yue, W. Wan, An investigation of ionospheric upper transition height variations at low and equatorial latitudes deduced from combined COSMIC and C/NOFS measurements, Adv. Space Res. 60 (8) (2017) 1617–1628.
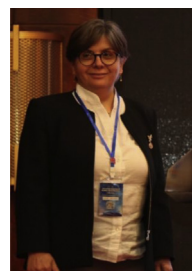
Arikan Feza was born in Sivrihisar, Turkey, in 1965. She received the B.Sc. degree (with high honors) in electrical and electronics engineering from Middle East Technical University, Ankara, Turkey, in 1986 and the M.S. and Ph.D. degrees in Electrical and Computer Engineering from Northeastern University, Boston, MA, USA in 1988 and 1992, respectively. Since 1993, she has been with the Department of Electrical and Electronics Engineering, Hacettepe University, Ankara, where she is currently a Full Professor. She is also the Director of the IONOLAB Group. Her current research interests include radar systems, HF propagation and communication, HF direction finding, Total Electron Content mapping and computerized ionospheric tomography. Prof. Arikan is a member of the IEEE, American Geophysical Union, COSPAR Commission C, chair of URSI-Turkey Commission G, and first Turkish member of IRI.